

Maximum Allowable Current Determination of RBS By Using a Directed Graph Model and Greedy Algorithm

Binghui Xu^{1†}, Guangbin Hua^{1†}, Cheng Qian^{1*}, Quan Xia^{1,2}, Bo Sun¹, Yi Ren¹, and
Zili Wang¹

¹School of Reliability and Systems Engineering, Beihang University, Beijing, 100191,
China

²School of Aeronautic Science and Engineering at Beihang University, Beijing, China

*Address correspondence to: cqian@buaa.edu.cn

[†]These authors contributed equally to this work.

Abstract

Reconfigurable ~~Battery Systems~~ battery systems (RBSs) present a promising alternative to traditional battery systems due to their flexible and dynamically changeable topological structure ~~subjected to that can be adapted to different~~ battery charging and discharging strategies. During ~~the operation of the RBS, the Maximum Allowable Current~~ RBS operation, the maximum allowable current (MAC) of the system that ensures ~~each battery that each battery's~~ current remains within a safe range ~~is a critical indicator to guide the system's reconfiguring control's reconfiguration~~, ensuring its safety and reliability. ~~In this paper, we firstly propose a calculation method for~~ This paper proposes a method to calculate the MAC of arbitrary ~~RBS~~ RBSs using a greedy algorithm in conjunction with a directed graph model of the RBS. ~~In this method, a new directed graph model is developed to model the structure of RBS, and a greedy algorithm is designed to find the possible circuit that enable MAC. Then, the MAC is calculated~~ By introducing the shortest path of the battery, the greedy algorithm transforms the enumeration of switch states in the brute-force algorithm into the combination of the shortest paths, which greatly increases the efficiency with which the MAC is determined. The directed graph model, based on the circuit-in-cooperate with the equivalent model of batteries and switches. The effectiveness of the equivalent circuit, provides a specific method for calculating the MAC of a given structure. The proposed method is validated by a novel and complex RBS on two published four-battery-RBSs and one with a more complex structure. The results show that this method is capable to calculated are the same as those of the brute-force algorithm, but the proposed method significantly improves the computational efficiency ($N_s 2^{N_s - N_b} \log_{10} N_b$ times faster than the brute force algorithm for an RBS with N_b batteries and N_s switches, theoretically). The main advantage of the proposed method is its ability to calculate the MAC of RBSs with ~~different structures or different battery sizes efficiently, which proves the correctness~~

~~of this method and its potential in facilitating next-generation RBS designs and applications, including battery isolation~~
arbitrary structures, even in scenarios with random isolated batteries.

1 Introduction

Battery ~~Energy Storage Systems~~energy storage systems (BESSs) are extensively ~~employed~~used in various applications, such as wind power plants and space power systems, to store and release high-quality electrical energy [1–5]. Typically, a BESS consists of numerous batteries interconnected by series-parallel circuitry to provide the required capacity storage. However, traditional BESSs, in which the batteries are connected in a fixed topology, ~~exhibit~~suffer from a significant weakness in their worst battery due to the so-called cask effect. Moreover, if ~~this~~the worst battery fails during operation, it ~~can~~is highly likely to exacerbate the degradation of ~~other batteries with a high possibility~~the other batteries, leading to reliability and safety issues [6–8]. These problems have become significant technical barriers in the development of new-generation space vehicles and ~~urgently~~need to be addressed [9].

Reconfigurable ~~Battery System (RBS)~~battery systems (RBSs), which can dynamically switch as required to different circuit ~~topology configurations as required, is~~topologies, are expected to solve ~~the above problems~~this problem [10]. The ~~ability of~~ switching circuit helps to isolate unhealthy batteries, ~~and thereby improve~~thereby improving the safety and reliability of the battery system. ~~Figure 1a shows~~To illustrate the working principle of an RBS, we consider a typical RBS structure developed by Visairo [11] ~~for dynamically adjusting the output voltage and current~~(Fig. 1a), which is taken as an example to show the reconfiguration process. In this structure, the batteries can be connected not only in series when the switches S_1 , S_5 , S_6 , S_7 , S_8 , S_9 , and S_{13} are closed (~~Figure 1b~~), ~~see Fig. 1b~~ but also in parallel when S_1 , S_2 , S_3 , S_4 , S_5 , S_9 , S_{10} , S_{11} , S_{12} , and S_{13} are closed (~~Figure Fig. 1c~~). Furthermore, when an unhealthy battery, for instance, the orange one B_3 in ~~Figure Fig. 1d~~, appears in the RBS, it can be isolated by opening its two adjacent switches (i.e., S_4 and S_{11}), ensuring ~~the system still remains that the system remains in~~ a reliable working mode.

~~The complex connection~~Recently, various types of RBSs with different flexibility and reconfigurability have been designed to meet application requirements. For example, Ci et al. [12] proposed an RBS structure that dynamically adjusts the battery discharge rate to fully exploit the available capacity of each battery. Jan's [13, 14] structures reconfigure structures with variant batteries in series to reach the (constantly changing) voltage requirements during electric vehicle charging. As shown in Fig. 1a, the structure proposed by Visairo et al. [11] changes the system's output voltage based on the load conditions, thereby reducing the power loss of the voltage regulator during the power supply process and improving the efficiency of energy use. Also, to enhance the energy efficiency of the system, Lawson et al. [15] and He et al. [16] proposed simplified structures that have fewer switches than Visairo's design. Kim et al. [17] improved the system's ability to recover from battery failures by introducing multiple ports into the structure.

The complex structure between batteries and switches ~~in the RBS provides~~gives RBSs flexibility but also ~~introduces challenges in design and operational control.~~ Unlike traditional BESSs with fixed outputs, the RBS output must be dynamically adjusted by controlling switch states to meet external

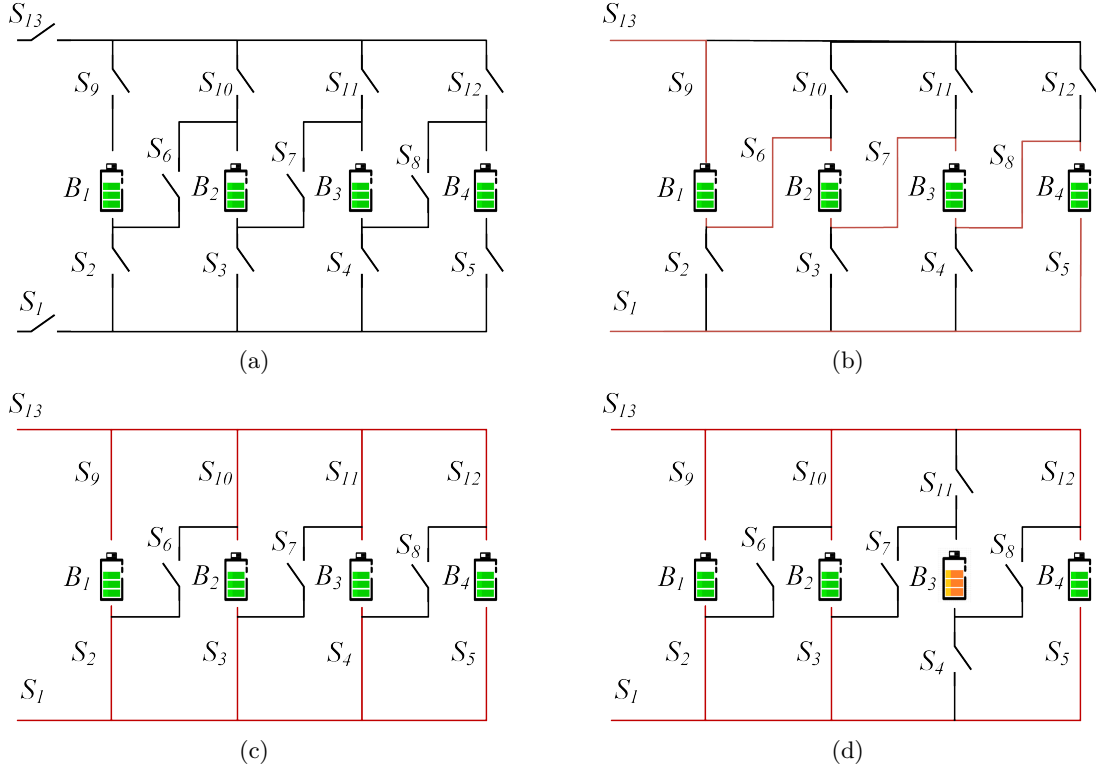


Figure 1: (a) The RBS structure proposed by Visairo[11], with all batteries in (b) series connection, (c) parallel connection, and (d) battery B_3 isolated.

load requirements. This necessitates additional, time-consuming output performance analysis during design and corresponding control strategies. An incorrect switch control strategy may cause battery short-circuiting or overload, risking the entire system. The Maximum Allowable Current creates challenges in the design and control of the system. Thus, several approaches to analyze the RBS structure and performance have been proposed to tackle these challenges. For instance, Han et al. [18] derived an analytical expression for the maximum switch current during battery system reconfiguration for a specific RBS structure. This helps guide the selection of switches and supports the design of RBS hardware. Chen et al. [19] proposed a systematic approach based on sneak circuit theory to fundamentally avoid the short-circuit problem of RBSs: They thoroughly analyzed all paths between the cathode and anode of each battery in the RBS and identified paths that only contain switches as short-circuit paths for pre-checking before system reconfiguration.

In spite of the maximum switch current mentioned above, the maximum allowable current (MAC), an RBS performance indicator, can guide designers in addressing this issue. MAC is defined as the maximum RBS output current that ensures each battery's current remains within a safe range. Therefore, it provides a benchmark for RBS output current, protecting individual batteries and identifying overall system output limits during operation. Despite its importance, no method currently exists for automatically evaluating MAC for RBSs. In particular, when one or more random cells are isolated, there is still no method to determine the MAC of the remaining RBS in time to assist the system in adjusting the control strategy timely. A universal and automatic method for calculating RBS MAC is urgently needed for practical applications. In this study, a directed graph model and greedy algorithm are employed to determine the MAC-allowed current under the constraints of the battery cell, is another critical indicator of RBSs that needs to be evaluated during the design or control of the system. The MAC helps the designers assess whether the RBS meets the output current requirements and contributes to the formulation of appropriate and safe management strategies for the battery management system. Unfortunately, few studies have analyzed the RBS structure to determine the RBS MAC. An intuitive and straightforward method is to enumerate all possible switch states and calculate the output current of the system under each reconfigured structure. However, this method is inefficient and time-consuming, especially for RBSs with a large number of switches.

To solve this issue, this paper proposes an efficient method to evaluate the MAC of RBSs. First, a greedy algorithm is designed to efficiently search the possible circuit topology of RBSs with MAC. Moreover, the method provides an improved direct graph model that considers the voltage, the internal resistance, the MAC of the battery, and the external load. The model obtains the accurate current of the RBS under a specific circuit topology. The main contributions of this paper can be summarized as follows:

- An efficient method is proposed to determine the MAC of RBS and the corresponding control strategy, effectively calculating the MAC for RBSs with arbitrary structures, including scenarios with isolated batteries.
- The greedy algorithm is applied to solve the MAC problem, the computational complexity of which is greatly reduced compared with the brute-force algorithm.

- An improved directed graph model is introduced; it considers the voltage, the internal resistance, the MAC of the battery, and the external load to analyze the current of the RBS.

The remainder of this paper is organized as follows: Section II presents the framework and details of the proposed directed graph model and the greedy algorithm. Section III demonstrated discusses a case study of using that uses the proposed method to determine the MAC of a novel and MACs of two published four-battery RBSs and one with a more complex structure. The calculation results, the algorithm's computational complexity, and scenarios such as batteries isolation also are battery random isolation are also discussed. Finally, the concluding remarks are drawn presented in Section IV.

2 Methodology

The central principle of this method is to make connect the batteries in RBS connected in parallel as much as an RBS in parallel to the extent possible, thereby maximizing the output current of the RBS. To achieve this universally and automatically achieve this, the overall process is divided into four steps, as shown in Figure 2. Firstly the four steps shown in Fig. 2. First, a directed graph model is established for subsequent computing, which computations. The model not only contains the connected relationships between batteries and switches, but also retains the performance parameters of the batteries. Subsequently, based on the equivalent circuit, the MAC problem is transformed into specific objective functions and constraints. Then, the The shortest paths (SPs, where additional batteries and switches on the path are penalized as distance) for the batteries are obtained then obtained by using the Dijkstra algorithm to guide connect the batteries in the RBS connect in parallel. Finally, a greedy algorithm is employed used to organize the switches, allowing the batteries to connect via their SPs while satisfying the constraints, resulting in the MAC of the RBS.

2.1 Directed graph Model model

He et al. [20] once proposed an abstracted directed graph model for an RBS, where the nodes represented represent the batteries, the edges represented represent the configuration flexibility, and the weight of each vertex corresponded corresponds to the battery voltage (Figure Fig. 3a). The model effectively captured captures all potential system configurations and offered offers a direct metric for configuration flexibility, but it did does not specify the physical implementation of the connectivity between batteries, meaning that one graph might have had correspond to multiple RBS structures. We previously proposed a novel directed graph model that, in contrast to differs completely from He's model, used by using nodes to represent the connections between batteries and switches, and directed edges to represent batteries and switches (Figure Fig. 3b), allowing for a one-to-one correspondence between the RBS structure and the directed graph model. This model was able to accurately and comprehensively represent represents the RBS topological structure but could not cannot be used for quantitative MAC calculations due to the lack of consideration for battery and switch performance parameters because it does not consider the voltage, internal resistance, and MAC of the battery. To address this, an improved directed graph model is used here

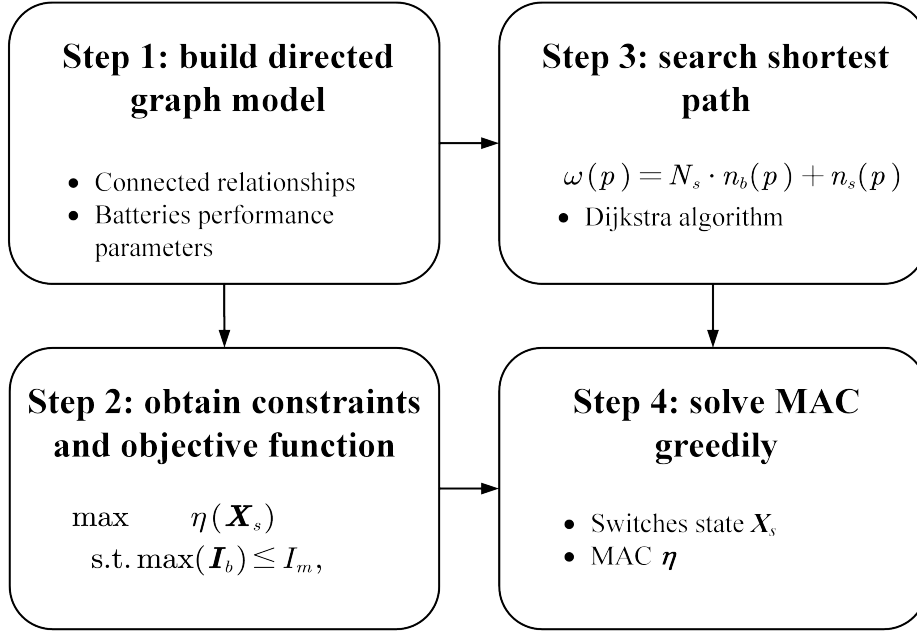


Figure 2: Diagram of this method, which contains four main steps.

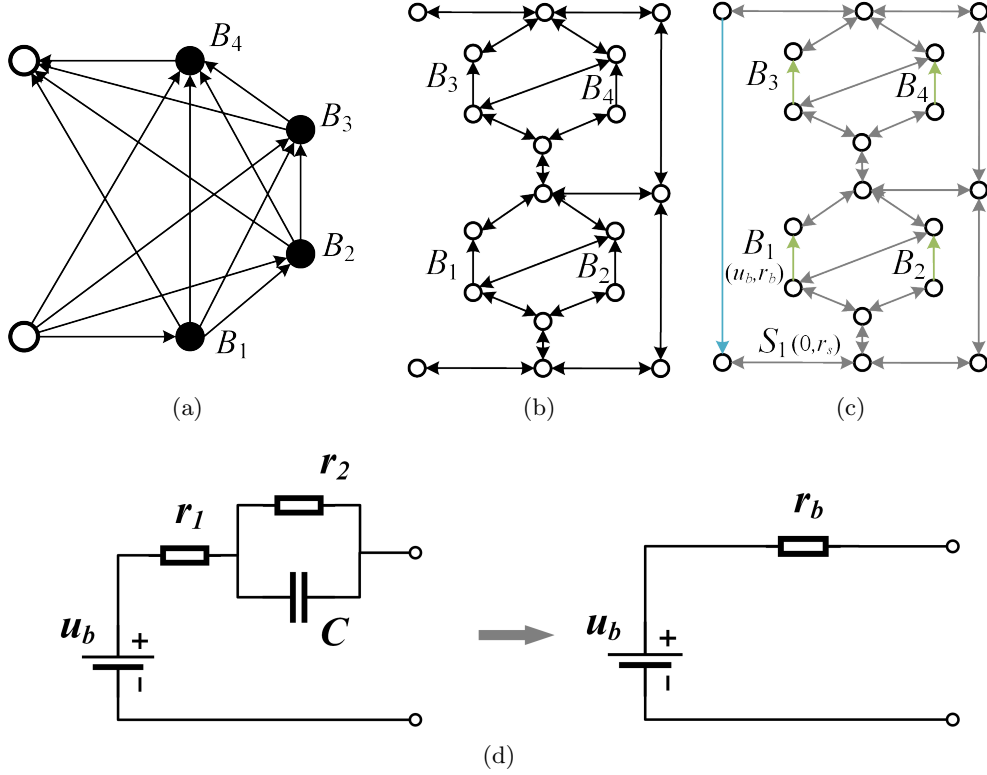


Figure 3: Directed graph models used in (a) He's work [20], (b) our previous work, and (c) [the improved model in](#) this paper. (d) The equivalent circuit of a battery in this method.

based on our original model, we improve our previous model by adding electromotive force and resistance attributes on the edges based to equivalent circuits(Figure 3e) on its equivalent circuits. The model also considers the external load as an equivalent resistance and integrate-integrates it into the analysis, making it a complete circuit model for later circuit analysis. The following will provide analyses. Fig. 3c shows the improved directed graph model used in this paper. The following provides a detailed explanation of the method for equating the components in RBS components in RBSs and constructing the directed graph model.

In order to use circuit analysis methods to solve the MAC of the RBS, the components in the RBS are equated to ideal circuit elements. As shown in Figure For instance, as shown in Fig. 3d, the battery in the RBS can be is represented as a black-box circuit consisting of two resistors (i.e., r_1 and r_2) and a capacitor (i.e., C), known as the Thevenin model [21, 22]. With an emphasis on the stable output of the RBS, the capacitor in the Thevenin model can be considered as an open circuit without affecting the steady-state current. Therefore, the battery B_i in the RBS can be simplified as the a series connection between a constant voltage source u_i and a resistor r_i . Furthermore, the state of switch S_j in the RBS is represented by a binary variable x_j , where 0 is for ON and 1 is for OFF, respectively OFF. When the switch is closed, it the circuit can be regarded as a resistor with a very small resistance value r_j . Lastly Finally, the external load is considered as a resistor with a value of resistance R_o .

For a given RBS structure, the its directed graph model for the RBS $G(V, E)$ is constructed as a directed graph $G(V, E)$ in such a way that follows:

1. Nodes: The nodes in the directed graph correspond to the connection points of components in the actual RBS. Assuming there are a total of N nodes in the RBS, for the sake of convenience, the anode of the RBS is denoted as v_1 and the cathode as v_N .
2. Edges: The edges in the directed graph correspond to the batteries, switches, and external electrical loads in the actual RBS. Therefore, there are three types of directed edges. For a battery B_i , its directed edge e_i is drawn from the cathode to the anode, as the battery because the battery in operation only allows current to flow in one direction when in operation. For a switch S_j , since it is allowed to work under bi-directional bidirectional currents, it is represented by a pair of directed edges with two-way directions. Regarding the external electronic load, as because it is connected to the anode and cathode of the RBS, a directed edge from v_N to v_1 is used to represent represents it. In conclusion, for a given RBS structure with N_b batteries and N_s switches, the total number of directed edges is $N_b + 2N_s + 1$, where 1 refers to the external electrical load.
3. Edges' attributes Attributes of edges: Each edge is assigned two attributes, voltage difference and resistance, based on the equivalent method mentioned above. The values for the battery B_i , switch S_j , and external loads correspond to (u_i, r_i) , $(0, r_j)$, and $(0, R_o)$, respectively.

2.2 Constraints and Objective Function objective function

187 ~~Based on the definition of MAC, determining the MAC of RBS~~ For a given RBS, determining its
 188 MAC involves maximizing the RBS output current while ensuring that ~~the currents of all batteries all~~
 189 battery currents do not exceed the batteries' ~~maximum allowable current. In this subsection, MAC.~~
 190 This subsection establishes the constraints and objective function to ~~solve~~ determine the RBS's
 191 MAC ~~will be established~~ through circuit analysis ~~, based on the previously constructed directed~~
 192 graph model provided in the previous section.

193 First, the topology in the directed graph model is represented in matrix form \mathbf{A} , known as the
 194 incidence matrix ~~, to facilitate circuit analysis. The specific definition of the incidence matrix is~~
 195 ~~shown in Equation 1.~~ and defined as follows:

$$a_{kl} = \begin{cases} 1, & \text{edge } l \text{ leaves node } k, \\ -1, & \text{edge } l \text{ enters node } k, \\ 0, & \text{otherwise.} \end{cases} \quad (1)$$

196 For a directed graph consisting of N nodes and $N_b + 2N_s + 1$ directed edges, its incidence matrix \mathbf{A}
 197 is an $N \times (N_b + 2N_s + 1)$ matrix. In this matrix, the rows and columns represent the nodes and edges
 198 of the directed graph, respectively. By distinguishing the components in the RBS corresponding to
 199 each column, \mathbf{A} can be rewritten as \div

$$\mathbf{A} = \begin{bmatrix} \mathbf{A}_b & \mathbf{A}_s & \mathbf{A}_o \end{bmatrix}, \quad (2)$$

200 where \mathbf{A}_b , \mathbf{A}_s , and \mathbf{A}_o are the ~~sub-matrices~~ submatrices corresponding to the batteries, switches,
 201 and external electrical load, respectively. To ~~alleviate~~ reduce the computational complexity, the
 202 dimensions of matrix \mathbf{A} ~~undergoes dimensionality reduction~~ are reduced. Since each directed edge
 203 has one node to leave and one to enter, the ~~sum of the~~ values in every column of \mathbf{A} ~~is~~ sum to zero.
 204 Therefore ~~removing any single one,~~ removing the last row will not result in a loss of information.
 205 ~~Without loss of generality, the last row is removed here. On the other hand, Conversely,~~ since each
 206 switch in the RBS is represented by a pair of directed edges with two-way directions, the two columns
 207 corresponding to the switch are mutually opposite. Thus, for the ~~sub-matrix~~ submatrix \mathbf{A}_s , only
 208 one column is retained for each pair of columns representing the same switch. As a result, \mathbf{A} can
 209 be reduced to ~~a~~ an $(N - 1) \times (N_b + N_s + 1)$ matrix, denoted ~~as~~ $\tilde{\mathbf{A}}$, for further calculation of current
 210 and voltage. Similar to ~~Equation 2~~ Eq. (2), $\tilde{\mathbf{A}}$ can be rewritten as \div

$$\tilde{\mathbf{A}} = \begin{bmatrix} \tilde{\mathbf{A}}_b & \tilde{\mathbf{A}}_s & \tilde{\mathbf{A}}_o \end{bmatrix}. \quad (3)$$

211 After obtaining the incidence matrix, the currents of all batteries and output in the RBS are
 212 determined by solving the circuit equations. According to ~~Kirchhoffs law~~ Kirchhoff's laws, we have

$$\begin{cases} \tilde{\mathbf{A}}\mathbf{I} = \mathbf{0}, \\ \mathbf{U} = \tilde{\mathbf{A}}^T \mathbf{U}_n, \end{cases} \quad (4)$$

where \mathbf{I} and \mathbf{U} indicate the current and voltage difference arrays of the $N_b + N_s + 1$ edges, respectively, and \mathbf{U}_n is the voltage array of the $N - 1$ nodes. These directed edges are treated as generalized branches and expressed in matrix form as follows:

$$\mathbf{I} = \mathbf{Y} \mathbf{X} \mathbf{U} - \mathbf{Y} \mathbf{X} \mathbf{U}_s + \mathbf{I}_s, \quad (5)$$

where \mathbf{U}_s and \mathbf{I}_s denote the source voltage and source current of the generalized branches, respectively. Because all batteries have been equivalent to voltage sources rather than current sources in the previous subsection, all elements of the array \mathbf{I}_s are 0, while zero, whereas the elements of the array \mathbf{U}_s are equal to the first attribute of the corresponding edges in the directed graph. The matrix \mathbf{Y} in Eq. (5) is the admittance matrix of the circuit, and is defined as the inverse of the impedance matrix. That is the elements of the diagonal. The elements on the diagonal of matrix \mathbf{Y} are equal to the reciprocal of the resistance, which is the second attribute of the corresponding edges in the directed graph, and the. The off-diagonal elements are 0. The of \mathbf{Y} are zero. \mathbf{X} is the state matrix, which describes that determines whether the RBS batteries and switches are allowed to can pass current. It is defined as

$$\mathbf{X} = \text{diag}(\underbrace{1, 0, \dots, 1}_{N_b \text{ of } 0/1}, \underbrace{1, 0, \dots, 1}_{N_s \text{ of } 0/1}, 1) = \begin{bmatrix} \mathbf{X}_b & & \\ & \mathbf{X}_s & \\ & & 1 \end{bmatrix}, \quad (6)$$

Where the elements where element x_i of the matrix \mathbf{X}_b represent whether the battery i indicates whether battery B_i has been removed from the circuit, with $x_i = 1$ indicating removal and $x_i = 0$ indicating that it battery B_i is still available to supply power. When all batteries are health healthy and capable of providing current to the external load, \mathbf{X}_b is an the identity matrix. The elements x_j of the matrix \mathbf{X}_s represent whether the switch j determine whether switch S_j is closed, with $x_j = 1$ indicating closure a closed switch and $x_j = 0$ indicating disconnection an open switch, which is consistent with the previous subsection.

Theoretically, the output current I_o and the currents of each battery \mathbf{I}_b in the RBS can be determined by solving Equations 4, 5, and 6 Eqs. (4)–(6) under any given state \mathbf{X} . In order to obtain specific constraint conditions and objective functions To further simplify the problem, it is further assumed that all batteries have the same electromotive force and internal resistance, denoted as which are denoted u_b and r_b , respectively. This allows for the derivation of us to derive explicit expressions for I_o and \mathbf{I}_b . After derivation and simplification, the output current I_o and the currents of each battery \mathbf{I}_b are ultimately represented as Equations 7 and 8, respectively. Eqs. (7) and (8) respectively:

$$I_o = \frac{1}{R_o r_b} \tilde{\mathbf{A}}_o^T \mathbf{Y}_n^{-1}(\mathbf{X}) \tilde{\mathbf{A}}_b \mathbf{U}_b, \quad (7)$$

$$\mathbf{I}_b = \frac{1}{r_b^2} [\tilde{\mathbf{A}}_b^T \mathbf{Y}_n^{-1}(\mathbf{X}) \tilde{\mathbf{A}}_b \mathbf{U}_b - r_b \mathbf{U}_b], \quad (8)$$

where \mathbf{U}_b is a $N_b \times 1$ array with all elements equaling equal to u_b , and \mathbf{Y}_n is the equivalent

admittance matrix of the circuit ~~and is~~ defined as

$$\mathbf{Y}_n(\mathbf{X}) = \frac{1}{R_o} \tilde{\mathbf{A}}_o \tilde{\mathbf{A}}_o^T + \frac{1}{r_b} \tilde{\mathbf{A}}_b \mathbf{X}_b \tilde{\mathbf{A}}_b^T + \frac{1}{r_s} \tilde{\mathbf{A}}_s \mathbf{X}_s \tilde{\mathbf{A}}_s^T. \quad (9)$$

To characterize the current output capacity of the RBS structure under different switching states, an indicator η is defined by the ratio of I_o ~~and to~~ $\max(\mathbf{I}_b)$ ~~shown in Equation 10:~~

$$\eta = \frac{I_o}{\max(\mathbf{I}_b)}. \quad (10)$$

Finally the problem of ~~solving finding the~~ MAC can be formulated as

$$\max \eta(\mathbf{X}_s) \quad (11)$$

$$\text{s.t.} \max(\mathbf{I}_b) \leq I_m, \quad (12)$$

where I_m is the ~~maximum allowable current~~ MAC of the battery.

However, it ~~is remains~~ computationally difficult to solve ~~11 because of the Eq. (11) because of~~ \mathbf{Y}_n^{-1} . On one hand, ~~due to~~ the introduction of nonlinear terms by \mathbf{Y}_n^{-1} , ~~many effective renders many~~ methods in linear optimization ~~are not suitable~~ ~~unsuitable~~ for this problem. On the other hand, the rank of \mathbf{Y}_n is proportional to the number of batteries and switches, which can be very large for a large RBS ~~system~~, leading to a significant computational burden. ~~Therefore~~ ~~As a result~~, intelligent algorithms that rely on ~~evolving evolution~~ by iteration may face efficiency ~~issues~~ ~~problems~~ when dealing with ~~large RBS system~~. ~~In order to a large RBS~~. To address this issue, the problem should be considered from the perspective of guiding the RBS to reconstruct as many parallel structures as possible. Consequently, a greedy algorithm based on the shortest path is proposed. The detailed implementation ~~process of this algorithm~~ is presented in the following two subsections.

2.3 Shortest ~~Path~~ ~~path~~

The path p used in this method is defined as the complete route that passes through one battery (or a consecutive series of batteries) and closed switches, connecting the anode v_1 to the cathode v_N of the RBS. By applying a penalty to the series-connected batteries on the path, where additional batteries imply a ~~longer~~ ~~greater~~ distance, the algorithm encourages the RBS to form parallel structures ~~as much as possible~~. ~~Meanwhile to the extent possible~~. ~~In addition~~, to reduce the number of switches controlled during the reconstruction process, a penalty is also applied to the total number of switches on the path ~~while ensuring the minimum number of batteries~~. Therefore, the distance ω of ~~the~~ path p is ~~defined by the following equation:-~~

$$\omega(p) = N_s \cdot n_b(p) + n_s(p), \quad (13)$$

where N_s is the total number of switches in the system, ~~and~~ $n_b(p)$ and $n_s(p)$ are number of batteries and switches in ~~the~~ path p , respectively. Moreover, the shortest path SP_i is defined as the path with

the minimum ω for battery i , as shown in the following equation B_i :

$$SP_i = \arg \min_{p \in P_i} \omega(p), \quad (14)$$

where P_i is the set of all paths from v_1 to v_N which pass through the that pass through directed edge i .

The SP_i can be solved by the Dijkstra algorithm. The Dijkstra algorithm is a graph-search graph-search method that finds the shortest path between two given nodes in a weighted graph, efficiently solving the single-source shortest-path problem. Assuming that shortest-path problem. Denoting the cathode and anode of battery i are denoted B_i as v_i^- and v_i^+ respectively, the then path p of battery i B_i can be divided into three segments: $v_1 \rightarrow v_i^-$, $v_i^+ \rightarrow v_N$, and $v_i^- \rightarrow v_i^+$. The $v_i^- \rightarrow v_i^+$ is the directed edge corresponding to battery i B_i . With the Dijkstra algorithm, shortest paths for the $v_1 \rightarrow v_i^-$ and $v_i^+ \rightarrow v_N$ can be calculated under the weights given in Equation 13, denoted as Eq. (13) and denoted $SP(v_i^- \rightarrow v_i^+)$ and $SP(v_i^+ \rightarrow v_N)$, respectively. Finally, the SP_i for battery i B_i is formed by the complete path with, which consists of $SP(v_1 \rightarrow v_i^-)$, $v_i^- \rightarrow v_i^+$, and $SP(v_i^+ \rightarrow v_N)$.

2.4 Greedy Algorithm

From the perspective of series vs parallel connections, integrating more batteries into the circuit through their shortest paths (SPs) results in a larger number of more batteries connected in parallel, thereby increasing the total output current of the RBS. However, conflicts may arise between the SPs of different batteries. For instance, the SPs of two batteries might form a short-circuited short-circuit RBS structure, which is not allowed. To address this issue, a greedy algorithm is employed to incorporate as many SPs incorporates as many SPs as possible while satisfying the reconstruction requirements.

The algorithm, as illustrated in Figure 4, can be (see pseudo-code in Algorithm 1) is illustrated in Fig. 4 and is summarized as follows, with the corresponding pseudo-code presented in Algorithm 1. First, the shortest paths (SPs) are obtained using Equations 13 and 14 SPs are obtained by using Eqs. (13) and (14) in conjunction with Dijkstra Search the Dijkstra search. Next, the matrix A is calculated using Equation 1 Eq. (1), and the initial N_{set} N_{set} is set to N_b . The algorithm iteratively checks uses a dichotomy method to iteratively check until convergence different combinations of c_b batteries from N_b and updates N_{set} using a dichotomy method until convergence is reached N_{set} . For each combination, the algorithm constructs an effective solution if possible, and calculates the currents I_o and I_b using Equations 7 and 8 by using Eqs. (7) and (8). If the maximum current I_b is less than or equal to I_m , the η is calculated using Equation 10 by using Eq. (10), and the maximum η is updated accordingly. Finally, the algorithm outputs the maximum η once N_{set} N_{set} converges.

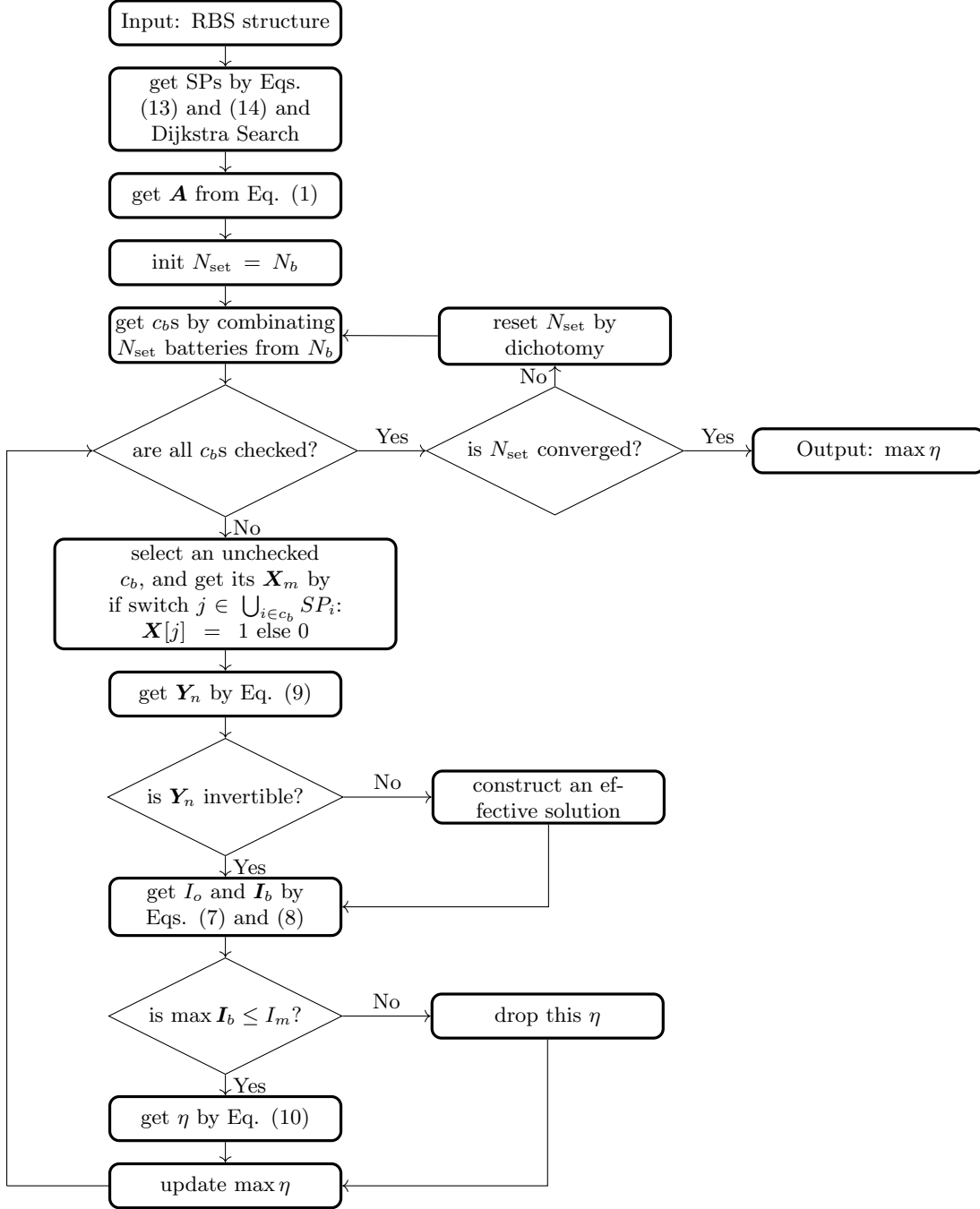


Figure 4: The computational flowchart of the MAC for a given RBS.

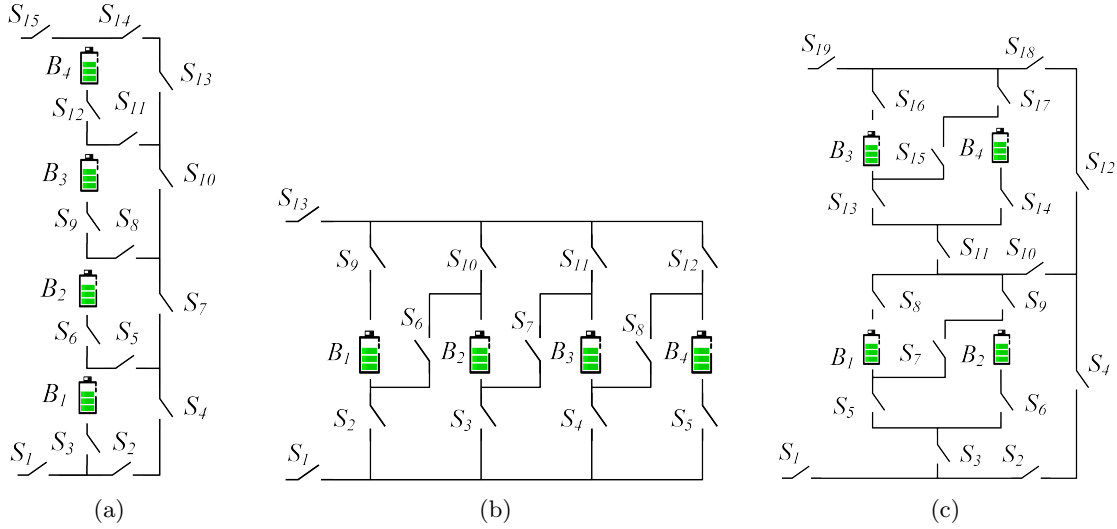


Figure 5: The ~~4-battery four-battery~~ RBS structures proposed by (a) Lawson [15], (b) Visairo [11], and (c) this paper.

3 Case Study

3.1 Structures

Currently, two types of RBS structures have been proposed by Visairo et al. [11] and Lawson et al. [15], both of which have ~~been applied in practice seen real use~~. The primary goal of Visairo's structure (Figure 5b) ~~was to achieve dynamic adjustment of RBS output ; however Fig. 5b) is to dynamically adjust the RBS output power. However~~, the isolation of unhealthy batteries ~~was is~~ not sufficiently addressed. ~~When batteries need to be isolated in the RBS of Visairo's structure, the methods for isolating them and the subsequent changes in RBS output warrant further investigation in their work.~~ Lawson et al. ~~conducted research on battery isolation in RBS and specifically designed the designed the RBS structure shown in Figure 5a . This structure has the advantage of easily isolating batteries, but Fig. 5a to isolate batteries. Although this structure easily isolates batteries,~~ it cannot dynamically adjust the output current of ~~the~~ RBS. Based on the structures of Visairo and Lawson, this paper ~~presents a new structure , as shown in Figure 5c, which combines the advantages of both proposes the structure shown in Fig. 5c.~~ By integrating the Visairo RBS structure into the Lawson RBS structure, the ~~new-proposed~~ structure not only ~~allows has~~ the flexibility to switch the batteries between series, parallel, and mixed series-parallel modes ~~, but also easily enables but also allows~~ the isolation of highly degraded batteries from the RBS. ~~And their variations in output current under battery isolation conditions will be studied. This RBS structure will be used to validate the effectiveness of the proposed method for calculating the MAC, and be compared with the Lawson's and Visairo's structure to illustrate its advantage on battery isolation~~ These four-battery RBS structures are investigated in the case study, including the scenarios with random isolated batteries.

3.2 Result

As shown in Figure Fig. 5c, the new RBS structure consists of 4 four batteries and 19 switches. The Figure 6a shows the corresponding directed graph is depicted in Figure 6a, which is composed of a total of 18 nodes and 43 edges. Batteries B_1 , B_2 , B_3 , and B_4 are denoted by green directed edges in the graph, while and the 19 switches are represented by gray directed edges with bi-directional bidirectional arrows. The external electrical load is treated as a directed edge from the cathode of the RBS (i.e., node 18) to the anode (i.e., node 1), as indicated by the blue directed edge in the graph. Utilizing Equation 13 Using Eq. (13) and the Dijkstra algorithm, the SPs SPs of the four batteries in the RBS structure of Figure Fig. 5c are highlighted by red in Figures 6b in red in Figs. 6b and 6e. Finally, the MAC calculation results calculated MACs of the structure in Figure 5c are shown as Table 1 and Figure 6f, Fig. 5c are listed in Tab. 1 and shown in Fig. 6f, as obtained by the greedy algorithm 1. Table Tab. 1 contains the switches states states of the switches, the output current I_o , the battery current I_b and, and the ratio η of the RBS structure with all batteries in good health when the RBS output reaches the MAC. Figure Fig. 6f presents the corresponding circuit, with the red highlight indicating that the current is flowing through the respective branches.

Table 1: Calculated MAC Calculating result of the 4-battery for four-battery RBS structure in Figure Fig. 5c.

Structure	Figure 5c with 4 four batteries and 19 switches
Switch ON-on	$S_1, S_3, S_5, S_6, S_8, S_9, S_{10}, S_{12}, S_{18}, S_{19}$
I_o	$2u_b/(2R_o + r_b)$
I_b	$[u_b/(2R_o + r_b), u_b/(2R_o + r_b), 0, 0]$
η max η	2

Similarly, the MAC calculation results of the structures in Figures MAC calculation for the structures in Figs. 5a and 5b are shown as Table 2 and Table listed in Tabs. 2 and 3, respectively.

To verify and compare the results from the greedy algorithm, we also used a brute-force algorithm that iterates through all possible switch states to calculate the MAC of the same three RBSs. The final results are the same as the results shown in Tabs. 1–3. The method uses the greedy algorithm to calculate 11, 11, and 1 reconfigured structures for the RBS structure in Figs. 5c, 5a, and 5b, respectively. For the same RBS, the method counts all possible switch states, which equates to 2^{19} , 2^{15} , and 2^{13} structures, respectively.

Table 2: MAC Calculating result of the 4-battery four-battery RBS structure in Figure Fig. 5a.

Structure	Figure 5a with 4 batteries and 15 switches
Switch ON	$S_1, S_3, S_5, S_7, S_{10}, S_{13}, S_{14}, S_{15}$
I_o	$u_b/(R_o + r_b)$
I_b	$[u_b/(R_o + r_b), 0, 0, 0]$
η max η	1

Furthermore, the RBS under the scenario of with isolated batteries is taken into consideration

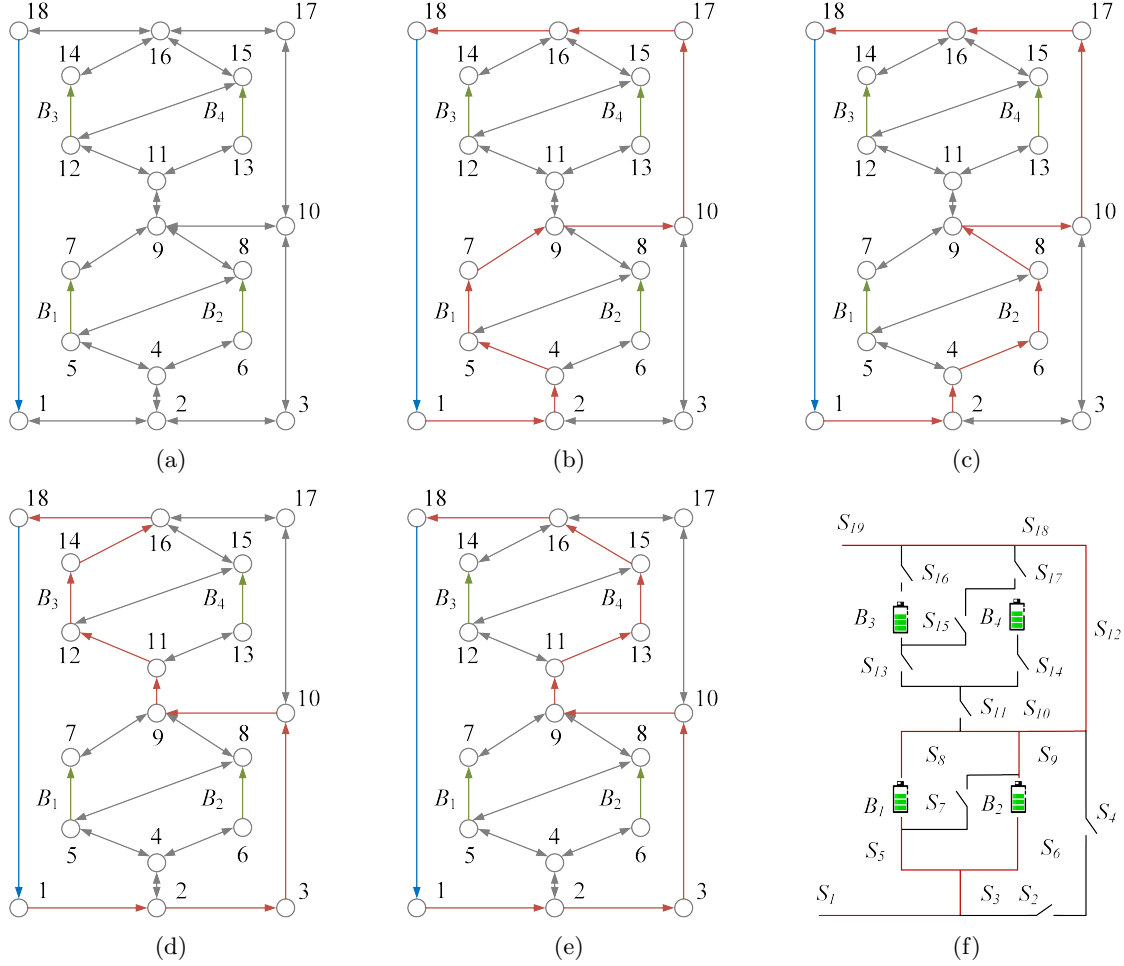


Figure 6: For the RBS structure in [Figure-Fig. 5c](#), (a) its directed graph and the ~~SPs~~ ~~SPs~~ (high-lighted in red) of battery (b) B_1 , (c) B_2 , (d) B_3 , and (e) B_4 . (f) ~~The circuit~~ ~~Circuit~~ of the RBS with its output reaching the MAC.

Table 3: MAC Calculating result of the ~~4-battery~~ ~~four-battery~~ RBS structure in [Figure-Fig. 5b](#).

Structure	Figure 5b with 4 batteries and 13 switches
Switch ON	$S_1, S_2, S_3, S_4, S_5, S_9, S_{10}, S_{11}, S_{12}, S_{13}$
I_o	$4u_b/(4R_o + r_b)$
I_b	$[u_b/(4R_o + r_b), u_b/(4R_o + r_b), u_b/(4R_o + r_b), u_b/(4R_o + r_b)]$
η max η	4

and calculated. The MAC calculation results for the three structures under study, with varying numbers of isolated batteries, are presented in Table 4. Figures 7a–7d illustrate the corresponding switch-control schemes for the new structure proposed in this paper under different isolated battery conditions. The characteristics of these three structures in the context of battery isolation will be discussed in the next subsection.

Table 4: Variation of MAC with the number of isolated batteries for different RBS structures, including the structure proposed by Lawson et al., Visairo et al., and the structure proposed in this paper.

Number of isolated batteries	η of RBS structure		
	our This paper	Visairo's	Lawson's
0	2	4	1
1	2	3	1
2	2 ^a or 1 ^b	2	1
3	1	1	1

^a Isolate two batteries within the same substructure, as shown in Fig. 7b.

^b Isolate one battery in each of the two substructures, as shown in Fig. 7c.

3.3 Discussion

In this subsection, we firstly discuss the correctness of the results presented in Figure 6 and Table 1. When B_1 and B_2 or B_3 and B_4 are connected in parallel, the RBS can output the maximum current, which is $\eta = 2$ (i.e., twice the current output of a single battery in the RBS). Adding more batteries to the main circuit can only form a series structure and will not improve the MAC. Therefore, the switches state given in Table 1 can make state of the switches given in Tab. 1 maximizes the RBS output current reach the maximum. The brute-force method, which go through all possible switch states, also gives the same result.

It is important to note that when solving for MAC the literature contains no report on an algorithm for calculating the MAC of an RBS. The brute-force algorithm, which goes through all possible switch states, is the most straightforward way to determine the MAC and is used as a benchmark for the proposed greedy algorithm. If an RBS has N_b batteries and N_s switches and the corresponding directed graph has N nodes, 2^{N_s} iterations are required to traverse all reconfigured structures. Calculating each reconfigured structure using Eqs. (7)–(10) requires matrix inversion and matrix multiplication, which has a time complexity of $O(N^3 + 2N^2N_b + N^2N_s + NN_b^2)$. Therefore, the time complexity of the brute-force algorithm is $O((N^3 + 2N^2N_b + N^2N_s + NN_b^2)2^{N_s})$. The greedy algorithm proposed in this paper requires that SP be found for each battery, which requires N_b iterations. Each SP can be obtained by several applications of Dijkstra's algorithms. Therefore, the total time complexity for calculating all SPs is $O(N_b(N_b + 2N_s)\log_{10} N)$. According to Appendix 1, the RBS can reconfigure $C_{N_b}^{N_{\text{set}}}$ structures by selecting N_{set} batteries from N_b batteries, which gives $\sum_{N_{\text{set}}=1}^{N_b} C_{N_b}^{N_{\text{set}}} / N_b \approx 2^{N_b} N_b^{-1}$ on average. Thus, with the bisection method, the time complexity of the greedy algorithm is $O((N^3 + 2N^2N_b + N^2N_s + NN_b^2)2^{N_b} N_b^{-1} \log_{10} N_b + N_b(N_b + 2N_s)\log_{10} N)$.

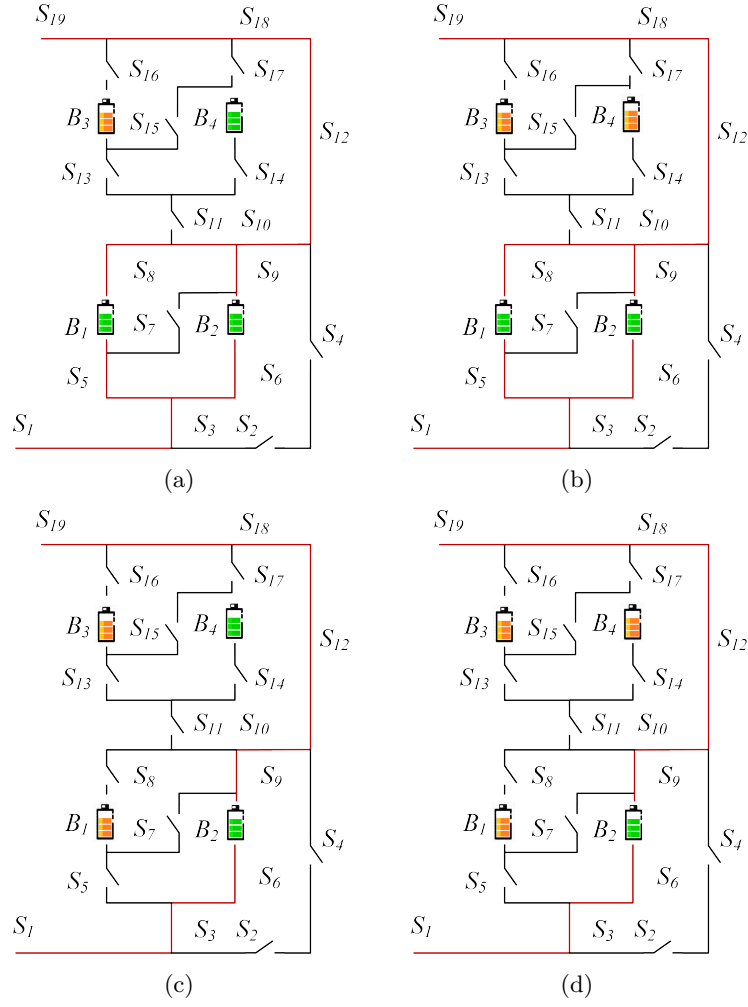


Figure 7: ~~The circuit~~ Circuit states of MACs when isolating (a) one, (b) two (best case), (c) two (worst case), and (d) three batteries for the structure in ~~Figure Fig.~~ Fig. 5c.

Based on currently proposed RBS structures [23–28], the number N_b of batteries, N_s of switches, and N of nodes are quantitatively related as follows: $N_s \approx (3-5)N_b$, $N \approx N_s$. After simplifying, the time complexity of the method with greedy algorithm is $O(2^{N_b} N_s^2 \log_{10} N_b)$, while it is $O(2^{N_s} N_s^3)$ for the method with brute force algorithm. Therefore, as the RBS grows, especially in the number of switches, the greedy algorithm gains an advantage over the brute-force algorithm. This is confirmed by the number of structures required to determine the MAC in the previous section. Compared with the brute-force algorithm, the method based on the greedy algorithm is 3 000 to 48 000 times more efficient, which is theoretically $N_s 2^{N_s - N_b} \log_{10} N_b$ times according to the above time-complexity analysis. This benefits from two key points:

- (1) The SPs guide the RBS to reconfigure reasonable structures rather than blindly going through all possible structures. This reduces the complexity from 2^{N_s} to 2^{N_b} , which is the main reason for the improvement in efficiency.
- (2) The bisection method further accelerates this process, reducing the complexity from 2^{N_b} to $2^{N_b} N_b^{-1} \log_{10} N_b$.

However, the greedy algorithm proposed in this paper still contains exponential terms in the time complexity, which means it may not be able to handle extremely large RBS structures having large N_b .

Note that η is used as the objective function instead of I_o in solving for the MAC. This choice makes the result of resulting MAC more reasonable. As shown in Table Tab. 1, I_o and I_b are functions of R_o , u_b , and r_b . If However, when I_o were is used as the objective function, even for the same RBS structure, the MAC result and corresponding switches state solution and corresponding switch states could change due to different external electrical appliances. If This would increase the difficulty and uncertainty in RBS structuredesign. In contrast, by using η as the objective function, which is defined as the ratio of I_o and $\max I_b$, the influence of these factors on the results can be eliminated. η solely reflects of designing the RBS structure. To eliminate this problem, the maximum output current capability of the RBS structure ratio $\eta = I_o / \max I_b$ is adopted as the objective function in our research. Recall that η reflects only the structure's ability to output current, rather than the actual current outputing by the battery system. Assuming that the maximum allowed current-MAC of batteries in the RBS is I_m , the maximum output current of the RBS structure can be calculated as ηI_m by determining the η of the structure. Therefore, compared to I_o , value of η is more suitable for structure design for the structure.

The method proposed in this paper is significant for facilitates the design of next-generation RBSs in the following aspects. Most of the ways: Most currently proposed RBS structures [23–28] exhibit have simple topological characteristics, and the calculation of so calculating the MACs is relatively straightforward, even intuitive. However, these simple structures do not always fully satisfy the requirements of complex applications, such as dynamically adapting the circuit to variable and random operating conditions, and/or actively equalizing differences among the between batteries in the RBS. Moreover, isolating the batteries disrupts the original regularity and symmetry of the topology, which complicates the otherwise simple structure, and the maximum output current of the system becomes more challenging to obtain. Owing to the advantages of pervasiveness and

~~automation~~In contrast, the proposed method ~~can be employed to calculate~~ calculates the MAC of arbitrary RBS structures, ~~which helps to address the aforementioned issues and paves the way for more notably the~~ complex and flexible RBS ~~structure design~~structures.

To illustrate this point, the MACs of ~~the~~ three RBS structures mentioned above are calculated after ~~the batteries are isolated~~isolating one or more of the batteries, as shown in ~~Table Tab.~~ 4. Specifically, for the structure presented in ~~Figure Fig.~~ 5c, the corresponding circuit states ~~of for the~~ MACs when isolating ~~different numbers of one to three~~ batteries are depicted in ~~Figures 7a-Figs. 7a-7d~~. This structure has two cases ~~of isolating two batteries in which two batteries are isolated:~~ one is to isolate two batteries within the same substructure (~~Figure Fig.~~ 7b), in which case $\eta = 2$; the other is to isolate one battery in each of the two substructures (~~Figure Fig.~~ 7c), in which case $\eta = 1$. ~~From the results, it can be observed~~The results in Figs. 7a-7d show that the proposed method provides reasonable outcomes for isolating ~~batteries with any number and position.~~

~~any number of batteries in any position.~~ Furthermore, the ~~performance of~~ output current for the three ~~RBS when isolating~~RBSs with isolated batteries is also shown in ~~Table Tab.~~ 4. For the structure proposed by Lawson et al., the MAC ~~remains the same as that without isolated battery cells, i.e., $\eta = 1$, when the~~ is independent of the number of isolated ~~battery cells increases, until all the cells in the RBS are isolated.~~ For batteries. However, for Visairo's structure, the MAC decreases ~~as upon increasing~~ the number of isolated ~~battery cells increases, until $\eta = 0$.~~ In contrast**batteries.** Nevertheless, the MAC of the structure proposed in this work ~~is positioned between the~~ falls between the MACs of these two structures. This ~~result~~ indicates that the structure proposed in this paper ~~, compared to Lawson's structure,~~ has a larger MAC ~~under than Lawson's for~~ the same number of batteries ~~, which means a wider output current regulation range.~~ On the other hand, by simply changing the states of S_2, S_4, S_{11} , and S_{12} in the conversion structure, this structure can address the majority of battery isolation scenarios, whereas Visairo's structure requires specific battery targeting and switch control. In summary, the structure proposed in this paper has the advantages of both ~~Lawson's and Visairo's structures~~and has a wider range of regulation of the output current.

4 Conclusion

This paper proposes a pervasive and ~~automatical method for computing~~ automated method to ~~efficiently compute~~ the MAC of ~~the given an~~ RBS. The method is implemented by a greedy algorithm combined with ~~a an improved~~ directed graph model, ~~whose effectiveness is tested on a novel and complex RBS structure.~~ The method remains effective for the application scenario of RBS battery isolation and demonstrates that the novel structure has the advantage on flexible output current and convenient battery isolation. Future research could focus on developing new indicators to evaluate the ~~performance.~~ The main advantage of this method is its ability to calculate the MAC of RBSs with arbitrary structures. Even in scenarios with random isolated batteries, the proposed method remains effective. The proposed method is more computationally efficient than the brute-force algorithm for the same calculation results, which is mainly because of using the batteries' SPs to guide the RBS to reconfigure reasonable structures rather than blindly going through all possible structures. This method helps to fully tap the current output potential of the RBS~~with the currents and voltages~~

obtained by the method, as well as modifying the equivalent model of the battery to allow for more accurate simulations of the RBS, including transient analysis, guide the RBS structure design and optimization in the design stage, and assist in evaluating the current-overload risk of the system in practical applications.

5 Appendix

Algorithm 1: Get the max available currents of a certain RBS

Data: Directed graph model $G(V, E)$ of the RBS
Result: $\max \eta$

```

1 for  $i \in E_b$  do
2    $P_i \leftarrow \{path | \text{starts at } v_1 \text{ and ends at } v_n\}$ ;
3    $SP_i \leftarrow p_i$  which has the minimum  $\omega(p_i)$  among all  $p_i \in P_i$ .
4 end
5 get  $A$  by Equation Eq. 1;
6 while not yet determine  $\max \eta$  do
7    $N_{set} \leftarrow$  number of selected  $SP$ s calculated by dichotomy  $N_{set} \leftarrow$  number of selected  $SP$ s
   calculated by dichotomy;
8    $C_b \leftarrow$  set of all combinations of  $N_{set}$  batteries from  $N_b$   $C_b \leftarrow$  set of all combinations of
    $N_{set}$  batteries from  $N_b$ ;
9   for  $c_b \in C_b$  do
10     $x_s \leftarrow$  list of all switches' state:  $x_s[j] = 1$  if  $j \in \bigcup_{i \in c_b} SP_i$  else 0;
11     $X \leftarrow diag[1, 1, \dots, 1, x_s]$ ;
12    get  $Y_n$  by Eq. 9;
13    if  $Y_n$  is invertible then
14      | pass
15    else
16      | construct an effective solution
17    end
18    get  $I_o$  by Eq. 7;
19    get  $I_b$  by Eq. 8;
20    if  $\max(I_b) \leq I_m$  then
21      |  $\eta \leftarrow I_o / \max(I_b)$ ;
22    else
23      | break
24    end
25  end
26 end

```

Acknowledgments

Author Contributions

B. Xu conceived the main idea, formulated the overarching research goals and aims, designed the algorithm, and reviewed and revised the manuscript. G. Hua developed and analyzed the model,

463 implemented the code and supporting algorithms, and wrote the initial draft. C. Qian provided
464 critical review, commentary, and revisions. Q. Xia contributed to shaping the research, analysis,
465 and manuscript. B. Sun conducted the research and investigation process. Y. Ren secured the
466 funding and supervised the project. Z. Wang verified the results and provided necessary resources.

467 Funding

468 This work was supported by the National Natural Science Foundation of China (NSFC, No.52075028).

469 Conflicts of Interest

470 The authors declare that there is no conflict of interest regarding the publication of this article.

471 Data Availability

472 This work does not require any data to be declared or publicly disclosed.

473 References

- 474 1. de Siqueira LMS and Peng W. Control Strategy to Smooth Wind Power Output Using Battery
475 Energy Storage System: A Review. *Journal of Energy Storage* 2021;35:102252.
- 476 2. Yang Y, Bremner S, Menictas C, and Kay M. Battery Energy Storage System Size Determin-
477 nation in Renewable Energy Systems: A Review. *Renewable and Sustainable Energy Reviews*
478 2018;91:109–25.
- 479 3. Cho J, Jeong S, and Kim Y. Commercial and Research Battery Technologies for Electrical
480 Energy Storage Applications. *Progress in Energy and Combustion Science* 2015;48:84–101.
- 481 4. Zhang L. Development and Prospect of Chinese Lunar Relay Communication Satellite. *Space:*
482 *Science & Technology* 2021;2021.
- 483 5. Schwanbeck E and Dalton P. International Space Station Lithium-ion Batteries for Primary
484 Electric Power System. In: *2019 European Space Power Conference (ESPC)*. IEEE, 2019:1–1.
485 DOI: 10.1109/ESPC.2019.8932009.
- 486 6. Yang N, Zhang X, Shang B, and Li G. Unbalanced Discharging and Aging Due to Temperature
487 Differences among the Cells in a Lithium-Ion Battery Pack with Parallel Combination. *Journal*
488 *of Power Sources* 2016;306:733–41.
- 489 7. Feng F, Hu X, Hu L, Hu F, Li Y, and Zhang L. Propagation Mechanisms and Diagnosis
490 of Parameter Inconsistency within Li-Ion Battery Packs. *Renewable and Sustainable Energy*
491 *Reviews* 2019;112:102–13.
- 492 8. Jeevarajan JA and Winchester C. Battery Safety Qualifications for Human Ratings. *Interface*
493 *magazine* 2012;21:51–5.

- 494 9. Pombo DV. A Hybrid Power System for a Permanent Colony on Mars. *Space: Science &*
495 *Technology* 2021;2021.
- 496 10. Han W, Wik T, Kersten A, Dong G, and Zou C. Next-Generation Battery Management Sys-
497 *tems: Dynamic Reconfiguration. IEEE Industrial Electronics Magazine* 2020;14:20–31.
- 498 11. Visairo H and Kumar P. A Reconfigurable Battery Pack for Improving Power Conversion
499 *Efficiency in Portable Devices. In: 2008 7th International Caribbean Conference on Devices,*
500 *Circuits and Systems. IEEE, 2008:1–6. DOI: 10.1109/ICDCS.2008.4542628.*
- 501 12. Ci S, Zhang J, Sharif H, and Alahmad M. A novel design of adaptive reconfigurable multicell
502 *battery for power-aware embedded networked sensing systems. In: IEEE GLOBECOM 2007-*
503 *IEEE Global Telecommunications Conference. IEEE. 2007:1043–7.*
- 504 13. Engelhardt J, Gabderakhmanova T, Rohde G, and Marinelli M. Reconfigurable Stationary
505 *Battery with Adaptive Cell Switching for Electric Vehicle Fast-Charging. In: 2020 55th In-*
506 *ternational Universities Power Engineering Conference (UPEC). 2020:1–6. DOI: 10.1109/*
507 *UPEC49904.2020.9209774.*
- 508 14. Engelhardt J, Zepter JM, Gabderakhmanova T, Rohde G, and Marinelli M. Double-string
509 *battery system with reconfigurable cell topology operated as a fast charging station for electric*
510 *vehicles. Energies* 2021;14:2414.
- 511 15. Lawson B. A Software Configurable Battery. EVS26 International Battery, Hybrid and Fuel
512 *Cell Electric Vehicle Symposium* 2012.
- 513 16. He L, Kong L, Lin S, et al. Reconfiguration-assisted charging in large-scale lithium-ion battery
514 *systems. In: 2014 ACM/IEEE International Conference on Cyber-Physical Systems (ICCPS).*
515 *IEEE. 2014:60–71.*
- 516 17. Kim H and Shin KG. On dynamic reconfiguration of a large-scale battery system. In: *2009 15th*
517 *IEEE Real-Time and Embedded Technology and Applications Symposium. IEEE. 2009:87–96.*
- 518 18. Han W, Kersten A, Zou C, Wik T, Huang X, and Dong G. Analysis and estimation of the max-
519 *imum switch current during battery system reconfiguration. IEEE Transactions on Industrial*
520 *Electronics* 2021;69:5931–41.
- 521 19. Chen SZ, Wang Y, Zhang G, Chang L, and Zhang Y. Sneak Circuit Theory Based Approach
522 *to Avoiding Short-Circuit Paths in Reconfigurable Battery Systems. IEEE Transactions on*
523 *Industrial Electronics* 2021;68:12353–63.
- 524 20. He L, Gu L, Kong L, Gu Y, Liu C, and He T. Exploring Adaptive Reconfiguration to Optimize
525 *Energy Efficiency in Large-Scale Battery Systems. In: 2013 IEEE 34th Real-Time Systems*
526 *Symposium. 2013:118–27. DOI: 10.1109/RTSS.2013.20.*
- 527 21. He H, Xiong R, Zhang X, Sun F, and Fan J. State-of-Charge Estimation of the Lithium-Ion
528 *Battery Using an Adaptive Extended Kalman Filter Based on an Improved Thevenin Model.*
529 *IEEE Transactions on Vehicular Technology* 2011;60:1461–9.
- 530 22. Mousavi G. S and Nikdel M. Various Battery Models for Various Simulation Studies and
531 *Applications. Renewable and Sustainable Energy Reviews* 2014;32:477–85.

- 532 23. Ci S, Zhang J, Sharif H, and Alahmad M. A Novel Design of Adaptive Reconfigurable Multicell
533 Battery for Power-Aware Embedded Networked Sensing Systems. In: *IEEE GLOBECOM 2007-
534 2007 IEEE Global Telecommunications Conference*. 2007:1043–7. DOI: 10.1109/GLOCOM.2007.
535 201.
- 536 24. Alahmad M, Hess H, Mojarradi M, West W, and Whitacre J. Battery Switch Array Sys-
537 tem with Application for JPL’s Rechargeable Micro-Scale Batteries. *Journal of Power Sources*
538 2008;177:566–78.
- 539 25. Kim H and Shin KG. Dependable, Efficient, Scalable Architecture for Management of Large-
540 Scale Batteries. In: *Proceedings of the 1st ACM/IEEE International Conference on Cyber-
541 Physical Systems*. ICCPS ’10. New York, NY, USA: Association for Computing Machinery,
542 2010:178–87. DOI: 10.1145/1795194.1795219.
- 543 26. Kim Y, Park S, Wang Y, et al. Balanced Reconfiguration of Storage Banks in a Hybrid Electrical
544 Energy Storage System. In: *2011 IEEE/ACM International Conference on Computer-Aided
545 Design (ICCAD)*. 2011:624–31. DOI: 10.1109/ICCAD.2011.6105395.
- 546 27. Kim T, Qiao W, and Qu L. A Series-Connected Self-Reconfigurable Multicell Battery Capable
547 of Safe and Effective Charging/Discharging and Balancing Operations. In: *2012 Twenty-Seventh
548 Annual IEEE Applied Power Electronics Conference and Exposition (APEC)*. 2012:2259–64.
549 DOI: 10.1109/APEC.2012.6166137.
- 550 28. He L, Kong L, Lin S, et al. Reconfiguration-Assisted Charging in Large-Scale Lithium-ion
551 Battery Systems. In: *2014 ACM/IEEE International Conference on Cyber-Physical Systems
552 (ICCPS)*. 2014:60–71. DOI: 10.1109/ICCPS.2014.6843711.